Oxygen Diffusion in Cu-based Catalysts: A Probe for Metal Support Interactions

Andrey V. Tarasov*[a], Alexander Yu. Klyushin[a] [b], Matthias Friedrich[a], Frank Girgsdies[a], Robert Schlögl[a] [c] and Elias Frei*[a]

[a] Dr. A. V. Tarasov , Dr. F. Girgsdies, Dr. A. Yu. Klyushin, Dr. M. Friedrich, , Prof. Dr. R. Schlögl, Dr. E. Frei
Department of Inorganic Chemistry
Fritz-Haber-Institut der Max-Planck-Gesellschaft
Faradayweg 4-6, 14195 Berlin (Germany)

[b] Dr. A. Yu. Klyushin
Helmholtz-Zentrum Berlin für Materialen und Energie GmbH,
BESSY II, Albert-Einstein-Straße 15, 12489 Berlin, (Germany)

[c] Prof. Dr. R. Schlögl
Max-Planck-Institut für Chemische Energiekonversion
Abteilung Heterogene Reaktionen
Stiftstr. 34-36, 45470 Mülheim an der Ruhr (Germany)

*Corresponding author:

Elias Frei, Andrey Tarasov: efrei@fhi-berlin.mpg.de, tarasov@fhi-berlin.mpg.de

Abstract

An extended N_2O titration method was applied to characterize high-performance, supported Cu catalysts: Cu/ZnO:Al (68/29/3), Cu/ZnO (80/20) and Cu/MgO (80/20). Calculation of the oxygen diffusion coefficients showed significant differences within the series of catalysts, particularly as a function of temperature. The diffusion kinetics follows a parabolic law similar to previous high temperatures studies. The apparent activation energies of the oxygen diffusion correlate inversely with the strength of the metal support interaction. The metal-support-interaction is described by means of complementary techniques as complex interplay between structural and electronic effects located at the Cu-metal oxide interface. The significance of the metal-support-interaction, identified as relevant for the reduction and oxidation of the metallic Cu, correlates with the activity in catalytic CO oxidation. It is evident that the oxygen diffusion coefficient is indicative of the tendency of the Cu catalyst to withstand transformation into the oxides under oxidative reaction conditions controlled by the corresponding Cu-support-interaction.

1. Introduction

Reactive nitrous oxide frontal (N_2O-RFC) or pulse chromatography is a well-established and standardized method [1] [2], that has been used for over 30 years in the characterization of Cu-based catalysts and in quantifying the Cu surface area [3]. Although this technique has often proved the linear correlation between surface area and activity in methanol synthesis, it fails to provide a correct interpretation of structure-function relationships for catalytic systems with strong Cu-ZnO interactions (i.e. where SMSI -strong metal support interaction- effects occur) [4-6]. Recently the presence of a "graphite-like" ZnO_x overlayer decorating the Cu particles in fresh and spent high-performance catalysts was clearly demonstrated by Lunkenbein *et al.* [7] [8]. The partially reduced ZnO_x layer influences adsorption properties of Cu and is indicative for the strong interfacial mediated interaction Cu/($Cu^{\delta+}$-*O*)-ZnO. In fact the oxygen vacancies in defective ZnO may contribute to more than 50% of N_2O capacity of such catalysts [9]. The relevance of the diffusion process has been perceived by Sato et al.[10] and is probably an inherent source of error in most of the N_2O-RFC experiments. Jensen et al.[11] proposed an improved N_2O-method for determining the Cu-dispersion. The surface and bulk oxidation of Cu-moieties are considered as separated processes, which explains the continuous detection of N_2. This N_2O-technique allows calculating the oxygen diffusion coefficients. To the best of our knowledge, it is the only published work where diffusion coefficients of oxygen in Cu have been measured for different Cu/Zn/Al catalysts[11]. This promising approach offers the accessibility of the oxygen mobility in metals (here: Cu) as key factor in red-ox dynamics of catalysts at elevated temperatures (when diffusion processes are pronounced). In other words, the resistance of a catalyst towards oxidation may affect the catalytic performance in oxidative reactions and possibly serves as a descriptor for phase stability and deactivation in general. In this respect, it remains unclear if the diffusional part of the N_2O profile may be indicative of the metal-support interaction, as represented e.g. by a ZnO_x overlayer on Cu particles in the Cu/ZnO:Al system [8, 12].

The effect of the support on oxidation resistance has been previously studied on Pt and Pd catalysts supported on a series of oxides by using pulse reaction N_2O decomposition below 300°C[13]. It is concluded that the acidic support affected the oxidation state of precious metals by promoting either the oxidation or the reduction step. It is expected that the Cu_2O growth front may be influenced by the metal-support interaction, as represented by e.g. Cu/($Cu^{\delta+}$-*O*)-ZnO interface, when the average thickness of the oxide film does not exceed values in the order

of 1-2 nm (as inferred from the dimensions of the ZnO_{1-x} overgrowth)[7, 8, 14]. In this region of thickness, rearrangement processes of surface domains, place exchange phenomena, electron transport and space-charge diffusion have an impact on Cu_2O-film growth[15]. In a recent study of Greiner *et al.*[16] the path of Cu catalysts surface corrosion during ethylene epoxidation was elaborately demonstrated and the relevance of Cu_2O and CuO on the reaction selectivity was shown.

Catalytic CO-oxidation was found to be a suitable test reaction for studying the metal-support interaction. The activity of a supported metal catalyst is known to depend e.g. on the reducibility of the support, an aspect that will also be addressed within this study. Higher activity as well as oxidative deactivation of the SMSI state were observed by investigating the light-off behavior in repeated temperature programmed cycles, as well as by isothermal measurements [17-19].

In the present article, we shed more light onto oxygen diffusion in Cu/metal oxide mixed catalysts. The corresponding oxygen diffusion coefficients were measured with N_2O-RFC on different high-performance catalysts (Cu/ZnO:Al, Cu/ZnO and Cu/MgO) and compared to reference samples also with respect to their apparent activation energies (E_a). To create a deeper understanding of the relevant processes during the N_2O reaction, *in-situ* X-ray diffraction (XRD), near edge X-ray absorption and photoemission spectroscopy (NEXAFS, XPS) were conducted. In order to find indicators for structure-function relationships of oxygen diffusion and SMSI, CO oxidation as suitable probe reaction was applied and thoroughly analyzed.

2. Experimental

2.1. Sample preparation

The studied catalysts were previously characterized and the detailed synthesis procedure was reported earlier. The synthesis protocol is based on co-precipitation using the concept of the industrial catalyst [20]. In brief, ZnO and Cu/ZnO (80/20) precursor were prepared by pH-controlled co-precipitation in an automated reactor (LabMax from Mettler-Toledo) at 65°C and pH=6.5 with subsequent calcination to the precatalyst in a rotating furnace at 603K for 3 h [21, 22]. A similar recipe was used for synthesizing the Cu/ZnO:Al (68/29/3) [23] and ZnO:Al (97/3) [24]. Impregnation of ZnO:Al was performed with 3g of pre-catalyst using 10g of Cu citrate dissolved in 30ml 12.5% ammonia solution, stirred for 3 days, dried at 120°C for 10h and calcined at 603K for 3 h in muffle furnace. The MgO and Cu/MgO (80/20) precursors were produced at pH=9. The obtained phase-pure Mg-substituted malachite precursor

$(Cu_{0.8}Mg_{0.2})(OH)_2CO_3$ was transformed into uniform material upon calcination at 603K according to [25]. The calcined MgO precatalyst was impregnated with 286 mg Cu-citrate in 2 ml diluted ammonia solution to yield Cu content of 10 mol-% dried and calcined at the same conditions as the pristine precursor. The 5wt-% Ag loaded Al_2O_3 was prepared by impregnation of $AgNO_3$ from aqueous solution with drying for 12h at 110°C and subsequent calcination at 400°C. A more detailed data on synthesis and structural characterization is given in the Supporting Information (Table S2).

2.2. Characterization Methods

N_2O chemisorption capacity was determined using reactive frontal chromatography (RFC) [26] in a custom designed temperature-programmed reaction setup. Approx. 100 mg of calcined sample (precatalyst) with 100-200 µm grain size was placed in a U-tube reactor with an inner diameter of 5 mm. The catalyst was positioned between two quartz-wool layers to form a thin bed. The in-situ reduction was performed at 6 K min^{-1}, 250°C, 30 min hold, with 80Nml min in 5%H_2 / Ar). The TPR profiles (Fig. S7) confirm the similarity of the catalysts regarding state, reducibility and amount of copper oxide in the precatalyst. The detailed microstructural characterization can be found elsewhere [25] [27]. After TPR the sample was cooled down in the reducing gas to a given temperature. It was subsequently flushed with helium to remove hydrogen completely. The gas phase composition was continuously monitored by mass-spectrometry, which also serves to assure that all traces of hydrogen are removed prior to the measurement. After stabilization of all intensities registered by MS the 1% N_2O in He mixture at 10 Nml min^{-1} was introduced by means of a four-way valve. In order to record a suitable titration profile for 5%Ag/Al_2O_3 a 0.1% N_2O in He was employed (Fig. S6). The N_2O chemisorption capacity and resulting apparent Cu surface area (Cu-SA_{N2O}) were calculated from the MS signal of the N_2 trace (m/z =28). The Mass-spectrometer was calibrated prior every measurement with 1% N_2 in He gas mixture. Contributions of fragments N_2^+ m/z=28, m/z=29 and N^+ m/z=14 were considered. On average, N_2O tests lasted around 90 min in order to monitor the diffusion tail of the N_2 profile. A fresh precatalyst batch was loaded for each measurement. Apparent Cu-SA_{N2O} were calculated assuming a stoichiometry of N_2:Cu 1:2, according to the surface reaction $N_2O + 2\ Cu \rightarrow Cu_2O + N_2$ and an average surface density of 1.47×10^{19} Cu-atoms m^{-2}. Ag-SA_{N2O} was calculated assuming stoichiometry N_2:Ag 1:2 and average surface density of 1.14×10^{19} Ag-atoms m^{-2} [28].The values are normalized to the

weight of precatalyst put into the reactor. The accuracy of the measurement is estimated with $\pm$ 1 m^2 g_{calc}^{-1}.

Sato et al. [10] pointed out the potential of the N_2O-RFC technique as a powerful tool for estimating Cu surface area under conditions where the catalyst support is not reduced in the TPR process. Nitrous oxide however tends to react with oxygen vacancies [6] [9] which were convincingly attributed to partially reduced ZnO_x [8, 9]. This holds for Cu/ZnO systems and is the main reason for the higher values of Cu surface area determined for ZnO containing Cu-based catalysts. For the calculation of diffusion coefficients of oxygen into the bulk of the copper, we used the true Cu surface area values determined by hydrogen transient adsorption (H_2-TA) technique as described by Kuld and co-authors [6] (Table S1).

Original N_2O curves have been transformed into square root time plots (O-$t^{1/2}$). The total amount of reacted oxygen, W, is represented by the sum of initial uptake by the surface reaction, $W_{surface}$, and the subsequent uptake caused from sub-surface diffusion, $W_{diffusion}$, when the surface concentration is constant. The diffusion coefficients have been calculated from the slope of the straight lines of the diffusional part of the curve, when $W_{surface}$ has been determined from the intercept. A graphical illustration of the process and details can be found in the respective sections of supplementary information (Fig. S1 and S2). Total oxygen content W pertains to the reaction of Cu_2O formation from the outer surface of the oxide towards the metallic bulk. The calculated diffusion coefficient D implies the molar flow of oxygen species through the cuprous oxide layer to the metallic center. This transport is driven by a linear gradient of oxygen concentration between the oxygen-oxide interface and metal boundary. According to theory of [29] [30] the oxide grows by diffusion of negatively charged [Cu^+] vacancies from the surface inward to the metal, accompanied by the flow of a positive electron holes and self -diffusion of copper ions by movement into the vacant sites. In other words the diffusivity D is proportional to the formation rate of Cu_2O growth and self-diffusion of Cu+ ions from the metal through the oxide.

It is worth noting the factors influencing the calculated diffusion coefficients, which are not accessible in a measurement, and are assumed to remain constant. The concentration of the diffusion species in the metal at the surface is equal to the gas concentration of N_2O rather than abundance O^{2-} in the solid phase. Furthermore, the possible changes of the Cu dispersion during oxidation could not be considered, especially at higher temperatures. Thus, it is presumed that the Cu surface area, and general surface morphology was constant and the catalyst maintained

the initial dispersion of the metal particles. The Cu surface area measured at RT before and after N_2O at 250°C differ by no more than 25%, depending on the sample. Moreover, the effect of grain boundary diffusion is neglected since diffusion coefficients for a selected number of samples of different sieve fractions show very modest variation within the statistical deviation interval. The formation of CuO oxide is unlikely since it forms at temperatures higher than 290°C as was shown by Fujita et. al. [31]. In spite of these ambiguities, we perceive that the region of applicability of the diffusion model is fair as long as linearity holds within parabolic coordinates.

H_2-transient adsorption (TA) was performed in the same setup that was used for N_2O-RFC and performed similarly as described in [6]. For approx. 100 mg of sample, H_2-TA was recorded at room temperature in 20 mL min^{-1}, 5% H_2 in Ar for one hour for the calcined sample (CuO), the reduced sample (Cu), and the sample after N_2O-RFC (Cu_2O) after a thorough purging in argon. Under the assumption that H_2 reacts only with surface Cu_2O, the areas between the Cu and Cu_2O transient adsorption branch was integrated, and the amount of consumed H_2 was quantified to deduce the Cu-$SA_{H2\text{-}TA}$ [24].

The in-situ XRD data were collected in Bragg-Brentano (divergent beam) geometry on a STOE Theta/theta X-ray diffractometer ($CuK\alpha_{1+2}$ radiation, secondary graphite monochromator, scintillation counter) equipped with an Anton Paar XRK 900 in-situ reactor chamber. The gas feed was mixed by means of Bronkhorst mass flow controllers, using helium as inert balance gas at a total flow rate of 100 mln/min. The effluent gas composition was monitored with a Pfeiffer OmniStar quadrupole mass spectrometer. The powder XRD data were analyzed and the lattice parameters calculated using a full pattern fitting, according to the Rietveld method as implemented in the TOPAS software (TOPAS version 5, © 1999−2014 Bruker AXS).

The reduced catalysts or precatalysts were characterized by near ambient pressure X-ray photoelectron spectroscopy (NAP-XPS) and X-ray absorption near edge spectroscopy (XANES). Measurements were performed at the ISISS-PGM beamline in the Helmholtz-Zentrum Berlin für Materialien und Energie – Electron storage ring BESSY II.[32, 33] A depth profiling experiment was performed in 0.25 mbar reaction mixture of the Cu 3p, Zn 3p and Al 2p core levels at photon energies of 255 and 1173 eV. The work functions were calculated from valence band and secondary electron cut-off measurements at 150 eV photon energy. In all XPS/NEXAFS experiments Cu-based catalysts were pelletized in self-standing discs mounted on a sapphire sample holder. Sample heating during the pretreatment and subsequent reaction

was achieved by an infrared laser. The precatalyst was first pressed in pellet, reduced in tube furnace and transferred under Ar atmosphere to the beam line in a airtight transfer chamber. For the *in-situ* N_2O-experiment, the catalysts were re-reduced in H_2 (0.5 mbar) at 250°C and 0.3 mbar and then cooled down to room temperature in UHV. Afterwards the catalysts were exposed to N_2O (0.5 mbar) and stepwise heated up to 250°C. NEXAFS spectra were collected at the Cu L_3-edge by analyzing the total electron yield (TEY). The overall spectral resolution was 0.3 eV in vicinity of Cu L_3-edge. Quantitative linear combination NEXAFS fitting was performed using the WinXAS software (http://www.winxas.de/)

The CO-oxidation, as a catalytic test reaction, was carried out in a custom-built catalytic reactor setup, described elsewhere [19]. The general procedure has been recently elaborated in [18, 19]. Usually, 25 mg of the precatalyst, diluted by 250 mg of inert SiC (250-355 µm) was positioned in the reactor. The sample was reduced at 250°C (5 Kpm) with 1h dwell time in 10% H_2. Subsequently three repeated light-off CO oxidation cycles were measured, with 2 °C min^{-1} in $CO:O_2:He=2:1:97=100$ Nml min^{-1}.

3. Results and Discussion

The diffusivity and solubility of oxygen in solid Cu has been studied in the temperature range from 600°C to 1000°C with potentiometric techniques [34, 35] and the kinetics has been measured to follow Ficks law. [36] Jensen *et al.* [11] proposed that the transport of oxygen during the N_2O-reaction at low temperatures occurs through O incorporation into Cu, thus the surface atoms of oxygen are steadily withdrawn from the surface by Fickian diffusion into the metal crystal lattice.[37] It is assumed that after surface saturation oxygen atoms are immediately replaced by new ones provided by N_2O molecules. Hence, the bulk oxidation process is considered as diffusion into a semi-infinite medium exposed to a constant surface concentration of the diffusing species, which are assumed to be limited by the N_2O concentration. Analogously to the study of Jensen *et al.*[11], a series of N_2O titration experiments has been performed on different supported catalysts [Cu/ZnO:Al (68/29/3), Cu/ZnO (80/20) and Cu/MgO (80/20), see also Table S1+S2, SI equation1 and Figure S1]. With Cu free supports or pure Cu powder no N_2O consumption in the RFC experiment has been detected [38]. Figure 1A shows a set of isothermal measurements of Cu/MgO (synthesis details, see experimental part). The Cu surface area measured in the temperature range 30-90°C varied between 21-25 m^2/g (grey-dotted lines), which agrees well with the H_2-TA value (24.9

m^2/g at 30°C for Cu/MgO). Consequently, this temperature region is identified as non-essential for subsurface diffusion. The area under the curve tail increases with increasing temperature. In accordance with previous studies [10, 39], the contribution of Cu_2O bulk formation through subsurface diffusion becomes significant at temperatures above 150°C. Plotting the data at various temperatures in coordinates of oxygen uptake versus $t^{1/2}$ an almost linear relation for the long time exposure is demonstrated, where W_s corresponds to the surface uptake (Figure 1B, see also Figure S2 for Cu/ZnO and Cu/ZnO:Al). This is also indicative for the applicability of the suggested diffusion model [40] mathematically described by Crank [41]. For all catalysts, a gradual increase of the oxygen diffusion rate with temperature is observed, leading to a tremendous acceleration in oxygen consumption at 250°C. Slower oxidation at the very beginning and a subsequent increase in diffusion rate implies a deviation from ideal straight lines. The scatter at moderate temperatures may appear due to very small crystallites, which cannot be considered to be of infinite dimensions. Consequently, the diffusion is hindered and the corresponding rates decrease. At higher temperatures, the increase in oxygen consumption rate is related with the disproportionation and aggregation of metal particles during oxidation. We may exclude catalytic N_2O decomposition since no signal of oxygen has been detected in the gas phase.

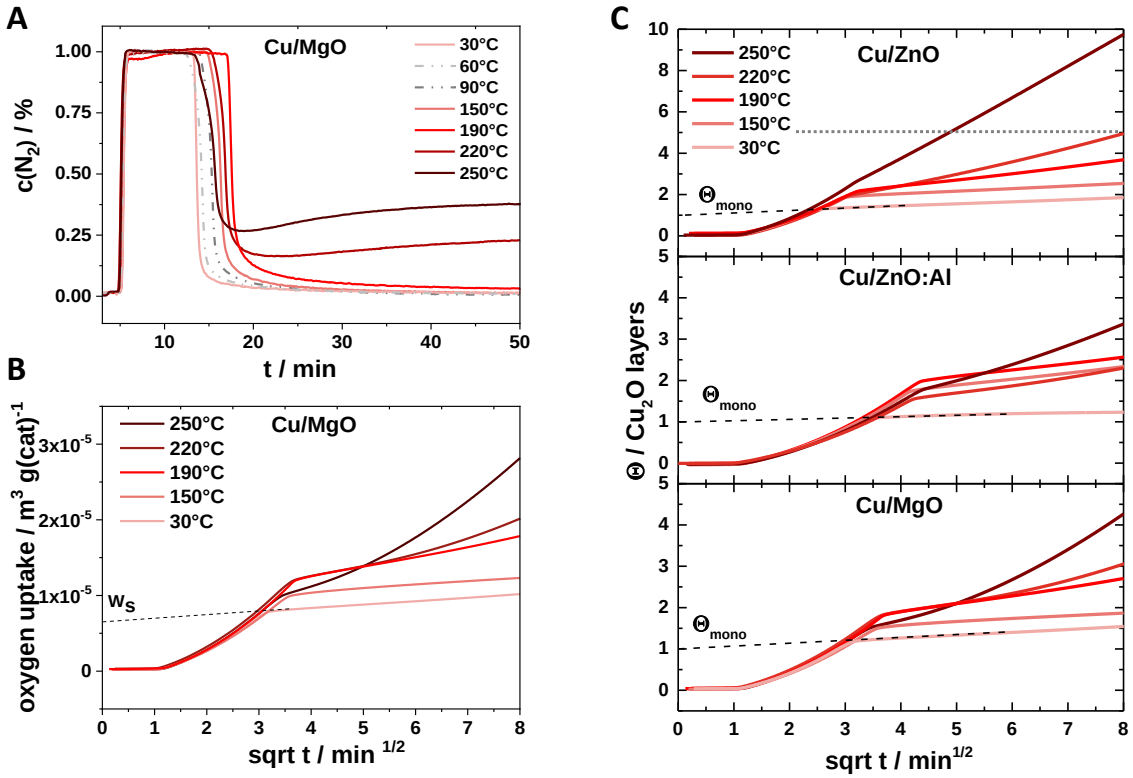

Figure 1. *Nitrogen concentration as a function of time at various temperatures on Cu/MgO catalyst (A). Oxygen uptake as a function of the square root of time exemplarily shown for Cu/MgO (B). Each*

run was carried out with a fresh sample. (100mg precatalyst, 10Nml min^{-1} 1%N_2O in He). Linearity in parabolic coordinates indicates the reaction by Fickian diffusion. Development of Cu_2O-surface front during N_2O titration (C). Grey dotted line for Cu/ZnO illustrates the size of the y-axis (five layers Cu_2O) of Cu/MgO and Cu/ZnO:Al as orientation. Cu/ZnO shows the fastest escalation of the oxide growth at temperatures above 150°C.

Figure 1C illustrates the development of a Cu_2O front during the catalysts oxidation with N_2O. Up to 190°C all catalyst possess similar thicknesses of Cu_2O front, not exceeding 3 layers. With increasing temperature, binary Cu/ZnO demonstrates continues acceleration of oxide growth, whereas for Cu/ZnO:Al and Cu/MgO the rate is slower. The resistance to oxidation is possibly related to the function of the support: **i.)** as a physical spacer between the Cu

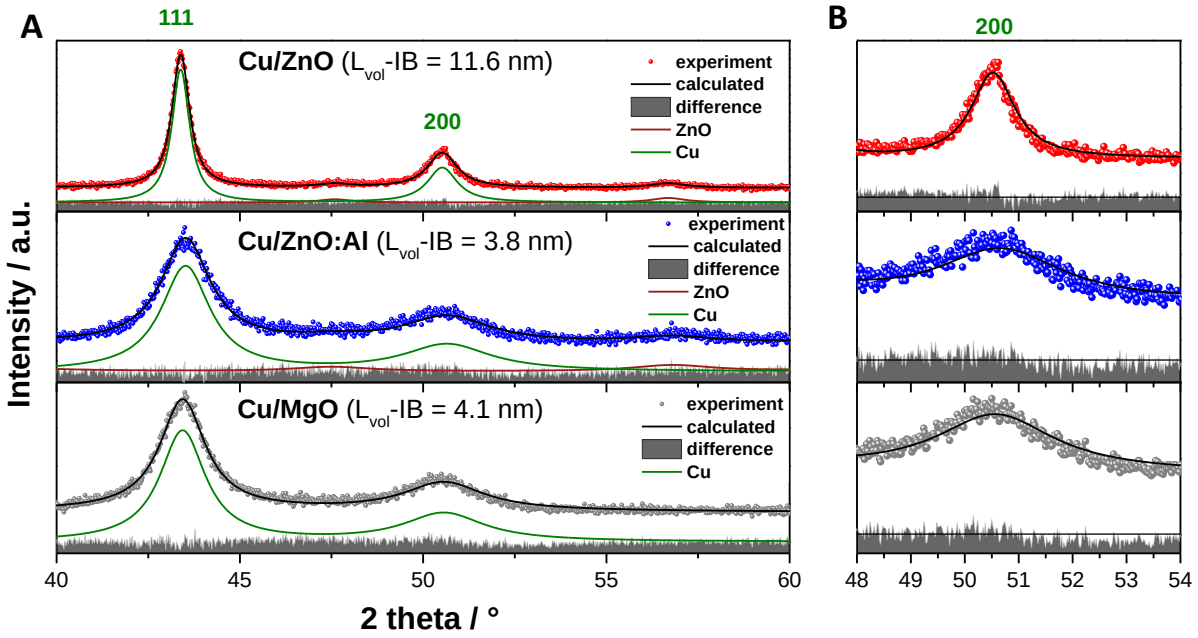

nanoparticles (discussed in the following as static metal-support interaction), stabilizing the porous microstructure; **ii.)** as a reducible and overgrowing species at the interfacial/perimeter contact to the Cu, affecting the adsorption properties (discussed in the following as dynamic metal-support interaction). An interplay of these effects is essential for the stabilization of the dispersed Cu [25]. A SMSI might be of static or dynamic nature.

Figure 2. *Rietveld fits of the reduced catalysts giving also the volume weighted domain sizes of the Cu crystallites (A). Zoom of the 200 reflection indicating qualitativly the Cu defectivity (B). The horizontal black line is a guide to the eye.*

To investigate a possible correlation of the oxygen diffusion/Cu_2O formation with the structural properties of Cu, *in-situ* XRD experiments were conducted. The precatalysts were at first *in-situ* activated under reductive atmosphere (5% H_2 in He) and analyzed. Figure 2A shows the diffraction patterns of Cu/ZnO (red), Cu/ZnO:Al (blue) and Cu/MgO (grey) with a magnification of the 200 reflection in Figure 2B. A quantitative analysis of the Cu phases evidences a significantly higher domain size for Cu/ZnO (11.6 nm) in comparison to

Cu/ZnO:Al (3.8 nm) and Cu/MgO (4.1 nm). This is a first indication for a difference in the Cu/metal oxide interaction, which is supported by a qualitative comparison of the peak shape of the 200 reflections (Fig. 2B). A general phenomenon observed in all three patterns is a pronounced peak broadening anisotropy, which leads to a proportionally stronger broadening of the 200 in comparison to the 111 reflection. In addition, the 200 peak exhibits an obvious shape asymmetry, with the lower angle flank being broader than the higher angle flank. Tentatively, we attribute both effects to the presence of stacking faults in the fcc lattice. While the model applied in the Rietveld fits successfully replicates the peak width anisotropy, the symmetric profiles used cannot describe the asymmetry. Thus, the systematic deviations seen in the difference curves of the 200 reflections (Fig. 2B) may serve as a qualitative indicator for the defective character of the Cu lattice. Due to the limited quality of *in-situ* XRD data, a quantitative evaluation is impossible (see also Fig. S3, normalized peak 220) [42]. The deviations are stronger pronounced for the Cu/ZnO:Al and Cu/MgO catalysts compared to Cu/ZnO, which is in line with the difference in Cu domain size, meaning that stronger Cu/metal oxide interaction leads to smaller and more defective Cu particles. This interpretation is emphasized by a particle size (PS) analysis from electron microscopy. Cu/MgO and Cu/ZnO:Al with a similar domain size show also similar mean PS (8.5±2.5 nm[25], respectively 8.1±2.6 nm[23]). A broad PS distribution with PS 5-50 nm[25] is obtained for the Cu/ZnO catalyst. It is suggested that SMSI, independent on its static or dynamic behavior, serve as descriptor for Cu domain and particle sizes and its microstructure (defectivity), respectively.

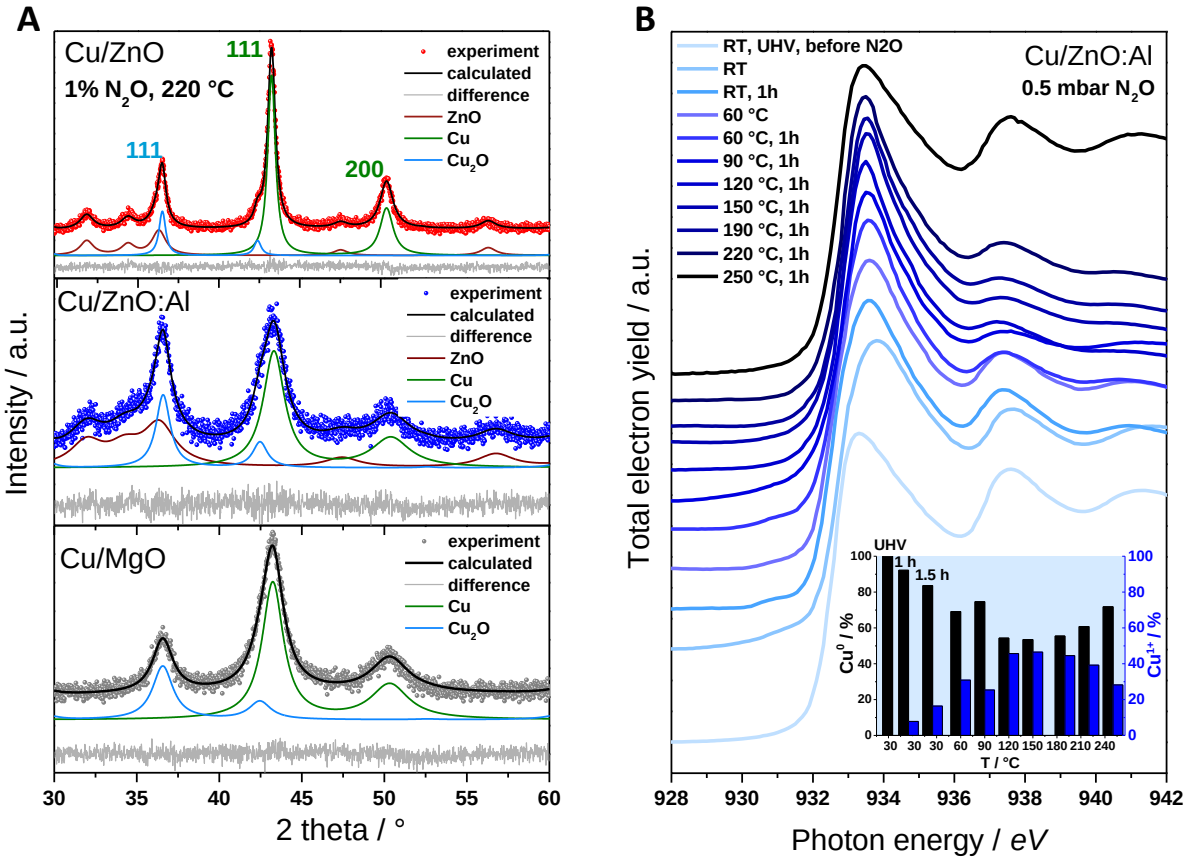

Figure 3. *In-situ XRD N_2O experiment of the catalyst at 220 °C analyzed by full pattern fitting (A). In-situ N_2O NEXAFS experiment of the Cu L_3-edge of Cu/ZnO:Al catalyst at various temperatures (B). The inset of (B) shows the amount of Cu^0 and Cu^{1+} from fitting based on linear combination of the reference spectra in Fig. S4 A and B.*

After reduction, the catalysts were *in-situ* analyzed by a similar N_2O experiment to Figure 1 (stepwise heating in a stream of 1% N_2O in He) by XRD and NEXAFS measurements. The *in-situ* XRD data in Figure 3A show a Rietveld analysis of the catalysts at 220 °C (below 220 °C no Cu_2O phase was detectable). The quantitative analysis of the full pattern fitting results is given in Table 1 as degree of oxidation, L_{vol}-IB of Cu_2O and strain (if needed). In comparison to Cu/MgO (5±2 nm) and Cu/ZnO:Al (6±2 nm), as already observed for the Cu domain size, the Cu_2O domain size of Cu/ZnO (17±10 nm) is distinctly increased. However, the relative increase with respect to the Cu domains is in the range of 50% for all samples. This indicates a correlation of the Cu domain sizes and the Cu_2O domains, in line with the process of oxide formation by the diffusion of Cu-ions to the surface [29, 30, 43]. Based on the phase ratio of Cu^0/Cu_2O the degree of oxidation by N_2O treatment is calculated. Using the Cu domain sizes extracted in Figure 2 and the degree of oxidation from Figure 3A and Table 1, an estimated number of Cu_2O layers is calculated (Table 1, see example of calculation SI Equ. 1). At 220 °C, the layer thickness of Cu_2O is similar for Cu/MgO and Cu/Zn:Al (~4 layers) and doubled for Cu/ZnO (~7-8 layers). The quantitative estimation of Cu_2O layers formation agrees well

with results gained from diffusion experiments in Figure 1, extrapolated to the time of XRD measurement (~2 hours). As a function of temperature, at 250 °C, the Cu_2O thickness grows significantly (compared to 220°C, ~ factor of 3) reflecting again the trends from oxygen diffusion experiments. To explain the experimental XRD patterns at 250 °C, microstrain broadening has to be included in the fit model of Cu_2O. The quantity of strain in Cu_2O is higher for Cu/MgO and Cu/ZnO:Al (0.0025) compared to Cu/ZnO (0.001). This is in line with the qualitative assessment of the Cu defectivity in Figure 2B and indicates a strong influence of the Cu_2O/metal-oxide interaction during the Cu_2O formation (SMSI induced defects) and a topotactic behavior. This means the defectivity of Cu_2O is predetermined by the defectivity of Cu as substrate and the growing mechanism of Cu_2O on top of Cu metal by Cu-ion diffusion. After 2h at 250 °C the catalysts are completely oxidized to Cu_2O. Analyzing the spent catalysts at RT gives Cu_2O domain sizes of 73 nm (strain 0.0012) for Cu/ZnO, 26 nm (strain 0.0027) for Cu/ZnO:Al and 19 nm (strain 0.0033) for Cu/MgO. This means an increase of the domain size from Cu to Cu_2O by a factor of ~5 (theoretically 1.2, Cu-Cu distance in Cu metal and Cu_2O, 0.25 vs. 0.3017 nm). Figure 3B shows the *in-situ* NEXAFS measurements at the Cu L_3-edge of the fully reduced Cu/ZnO:Al catalyst at various temperatures under a partial pressure of 0.5.mbar (~half of the *in-situ* XRD experiment). The white-line at 933 eV and the post-oscillations are indicative for the oxidation state of Cu.[44] The inset of Figure 3B gives the amount of Cu^0 and Cu^{1+} from fitting analysis (see also Fig. S4A and B, reference spectra). At RT, with surface sensitive NEXAFS measurement, a distinct oxidation, stabilizing at ~17% Cu_2O, is already visible. As a function of the temperature the Cu_2O ratio incrementally increases to a maximum of ~47% at 150 °C and finally decreases again. After 1h at 250 °C, the Cu_2O moieties stabilize at 28%. Calculating, based on the degree of oxidation from NEXAFS data and the determined Cu domain size, an estimated layer thickness of Cu_2O at 250°C, the resulting 3-4 layers correspond exactly to the values obtained from the oxygen diffusion experiment in Figure 1C (Cu/ZnO:Al system, 250 °C). However, the discontinous development of Cu_2O emphasizes the complex processes of adsorption, diffusion and ion mobility occuring during the experiment. Besides, these processes are controlled by the intrinsic properties of the material (e.g. defectivity of Cu and SMSI) and extrinsic influences (temperature and the chemical potential of the gas phase).

Table 1. *Fit results and calculation of the Cu_2O layer thickness of Cu/ZnO, Cu/ZnO:Al and Cu/MgO at different temperatures under an atmosphere of 1%N_2O in He.*

	Cu/ZnO	**Cu/ZnO:Al**	**Cu/MgO**	**T / °C**

[a]$Cu^{0} \rightarrow Cu^{1+}$ / %	17	29	27	**220**
[b]L_{vol}-IB / nm	17 ± 10	6 ± 2	5 ± 2	
[c]Cu_2O / layers	6.5[*]→7.9	3.7[*]→ 4.4	3.7[*]→ 4.4	
$Cu^{0} \rightarrow Cu^{1+}$ / %	55	76	68	**250**
L_{vol}-IB / nm	32 ± 9	16 ± 6	10 ± 2	
Cu_2O / layers	21.1 → 25.5[*]	9.6 → 11.6[*]	9.2 →11.2[*]	
strain	0.001 ± 0.0003	0.0025 ± 0.0008	0.0025 ± 0.0007	
$Cu^{0} \rightarrow Cu^{1+}$ / %	99	100	100	**RT (spent)**
L_{vol}-IB / nm	73 ± 7	26 ± 10	19 ± 5	
strain	0.0012	0.0027 ± 0.0005	0.0033 ± 0.0005	

[a] degree of Cu metal oxidation calculated from the XRD fits, Fig. 3

[b] volume weighted Cu_2O domain size from *in-situ* XRD measurements

[c] Cu_2O layers calculated from the Cu domain size from Fig. 2 with respect to [a] and Cu-Cu distance of 0.25 nm for Cu metal based calculations [*] or Cu-Cu distances of 0.3017 nm for Cu_2O based calculations (see Figure S5)

To elucidate and quantify the role of the support on the dynamics of Cu oxidation, the diffusion coefficients of oxygen have been calculated in the temperature range of 30-250°C (see also Fig. S1 and SI). Table S1 summarizes the values of diffusion coefficients of three catalyst families. The results are presented in Figure 4A. The diffusion coefficients of all catalysts grow continuously with temperature. At 30°C the diffusion coefficients are low and start to increase significantly at 220 °C. The diffusion coefficient of Cu/ZnO at 220 °C is ~4 times higher compared to Cu/ZnO:Al. Obviously, the incorporation of Al into the lattice of ZnO (as dopant with an influence on e.g. oxygen vacancies and SMSI) [8, 24] has a huge impact on the interaction to the Cu nanostructure. This means, the higher reducibility of the ZnO:Al support at the interfacial contact to Cu leads to a better incorporation [44] (ZnO overlayer) and stabilization of the Cu moieties (particle size and strain induced defects) with direct consequences on the oxygen diffusion coefficients. To demonstrate the correlation of the oxygen diffusion coefficient and the metal-support interaction, an impregnated catalyst with 10 wt.-% Cu on ZnO:Al was investigated (blue-and-orange point in Fig. 4A). This system mimics an intended loss of metal-support interaction and features a 3.5-times higher diffusion coefficient at 250°C as compared to the co-precipitated one (Table S1 and Fig.4A, dashed orange arrow). In contrast, Cu/MgO shows at 250 °C a 5.5-times lower diffusion coefficient than Cu/ZnO:Al, although the Cu nanostructures are directly comparable (Fig. 2). This means the non-reducible support MgO exhibits a strong static interaction to Cu, stabilizing the domain

size and defects without any tendencies to overgrow [25]. In that respect, the overgrowth of the ZnOx [7, 8] does not render as protection layer preventing O diffusion, but rather has a stabilization function for the defective Cu nanoparticles. Moreover, the non-static and reducible ZnO support promotes the oxygen diffusion.

Analysis of adhesion energies for Cu particles below 10nm on crystal faces MgO(100) (E_{adh}=1.9 J/m^2) [45] and ZnO(0001) (E_{adh}=3.4 J/m^2) [46] suggests however stronger anchoring of Cu to ZnO than to MgO surface. On the other hand, oxygen vacancies on partially reduced surface layer of ZnO weaken significantly the Cu/ZnOx interface energy (E_{adh}= 0.9-1.4 J/m^2) as demonstrated for supported catalysts [47, 48]. Considering the results of single crystal studies on MgO (100) [49-51], the certain stabilization of metal/oxide bonding may be a result of surface hydroxyls which in turn may lead to the increase of adhesion on Cu/MgO interface. Comparing the oxygen diffusion coefficient of coprecipitated Cu/MgO to an impregnated catalyst with 10 wt.-% Cu on MgO, leads anew to an increase by a factor of ~5 (Fig. 4A grey-orange point and Table S1) as a direct result of the metal-support interaction loss.

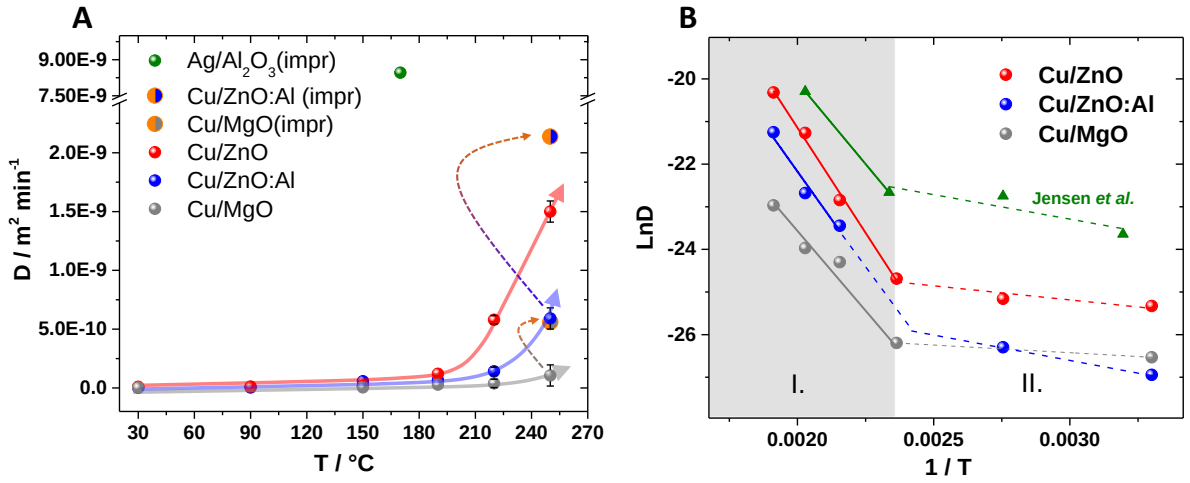

Figure 4. *Change of oxygen diffusion coefficient with temperature for various co-precipitated and impregnated catalysts (A). Arrhenius plots of selected catalysts (B).*

A reference measurement with supported Ag/Al_2O_3 (Figure S6) validated the reliability of the diffusivities (Table S1). The low oxophilicity of Ag combined with its larger lattice parameter of 4.086Å (compared to Cu=3.615Å) results in a vastly growing diffusion coefficient, already at lower temperatures (Table S1, Fig. 4A green point) [35] [52] [53].

Since the diffusion experiments were performed at various temperatures, the corresponding apparent activation energies (E_a) for the oxygen diffusion process are calculated. Figure 4B illustrates the relevant Arrhenius plots of the LnD vs. the inverse temperature. The different slopes at high temperature (region I.) and low temperatures (region II.) indicate that also

different E_a respectively processes are involved. In the temperature region below 150°C a formation of thin Cu_2O film ceases the oxidation [54]. The process is limited by adsorption [55] and ionic transport on $Cu_2O_{surface}/Cu_{bulk}$ interface. Further supported by the low activation energies in the range of 10-20 kJ/mol, energies where e.g. adsorption-desorption processes are described [15]. With increasing temperature, the formation of a Cu_2O layer develops in terms of a parabolic law. Homogeneous-field and space-charge-modified diffusion can be expected to predominate [15], in accordance to high temperature experiments of Wagner *et al.*, suggesting a mechanism governed by diffusion of Cu-ions [43] [29]. This interpretation is convincingly vindicated by Bardeen et al. [30], identifying the diffusion of Cu^+ vacancies from the outer surface of the oxide towards the metal by radioactive Cu tracer experiments. The activation energies for oxygen diffusion in solid Cu or electrochemical high temperature studies on bulk Cu at 600-1000°C varies in the range of ~60-80 kJ/mol [34-36, 56] (Table 2).

Table 2. *Apparent activation energies and pre-exponential factors for oxygen diffusion.*

Reference	Temperature / °C	A / m^2 min^{-1}	E_a / kJ mol^{-1}
Albert and Kirchem[36]	620-1000	$5.8*10^{-5}$	61.2
Pasorek and Rapp[56]	700-1000	-	67.2
Narula *et al.*[34]	700-1000	$7.0*10^{-5}$	67.3
Ramanarayanan and Worrell[35]	800-1000	$14.4*10^{-5}$	78.1
Cu/ZnO/Al, Jensen *et al.*[11]	150-220	$9*10^{-2}$	63.9
Cu/ZnO	150-250	$2.4*10^{-1}$	82±4
Cu/ZnO:Al	190-250	$1.7*10^{-2}$	75±15
Cu/MgO	150-250	$4.7*10^{-5}$	62±7

These values are in very good agreement with the E_a calculated for Cu/ZnO (82 kJ/mol), Cu/ZnO:Al (75 kJ/mol) and Cu/MgO (62 kJ/mol), which constitutes that the oxygen diffusion in Cu supported catalyst at moderate temperatures (150-250 °C) likely follows the same kinetics as in bulk Cu at the high temperature range. The increase of the E_a, inverse to the strength of the Cu support interaction (less impact of the temperature) evidencing the probing character of the oxygen diffusion coefficient. In other words, a stronger Cu support interaction leads to smaller and more defective Cu particles where oxygen diffusion occurs with a comparably low E_a and less involved diffusion sites/channels (small diffusion coefficients at high temperatures of e.g $59 \cdot 10^{-11}$ m^2 min^{-1} at 250 °C for Cu/ZnO:Al). The less defective and

bigger Cu moieties in Cu/ZnO offer (see also Figure 2B), very likely, more diffusion sites/channels with higher E_a (large diffusion coefficients of e.g. $150 \cdot 10^{-11}$ m^2 min^{-1} at 250 °C).

The metal support interaction plays obviously a major role with respect to the metal dispersion, its defectiveness (also reflected in the formed Cu_2O) and as a consequence for the oxygen diffusion properties. Since the catalytic CO oxidation serves as a suitable tool for the analysis of SMSI[17-19], three consecutive cycles (light-off curves) on the Cu/MgO, Cu/ZnO and Cu/ZnO:Al samples were applied (Figure 5A). Prior to the testing period, all catalyst were activated under reductive atmosphere (5% H_2 in Ar, Figure S7) [44]. Cu/MgO and Cu/ZnO:Al show (e.g. at 50% conversion) a shift to higher temperatures (deactivation) between the first and second cycle and a stabilization between the second and the third one. This stabilization effect is also visible for the Cu/ZnO catalyst; however, the first cycle shows a "saddle-like" profile distinctly different from the others. Such an activation curve was already observed on Cu-ZnO model systems tentatively interpreted as oxidation event [17] or on Cu single crystals as surface roughening under the formation of an amorphous CuO_x layer [57]. This indicates a possible oxidation of the Cu moieties in the CO oxidation responsible for the saddle-like profile (Cu/ZnO) and the deactivation (Cu/MgO, Cu/ZnO:Al) during cycling.

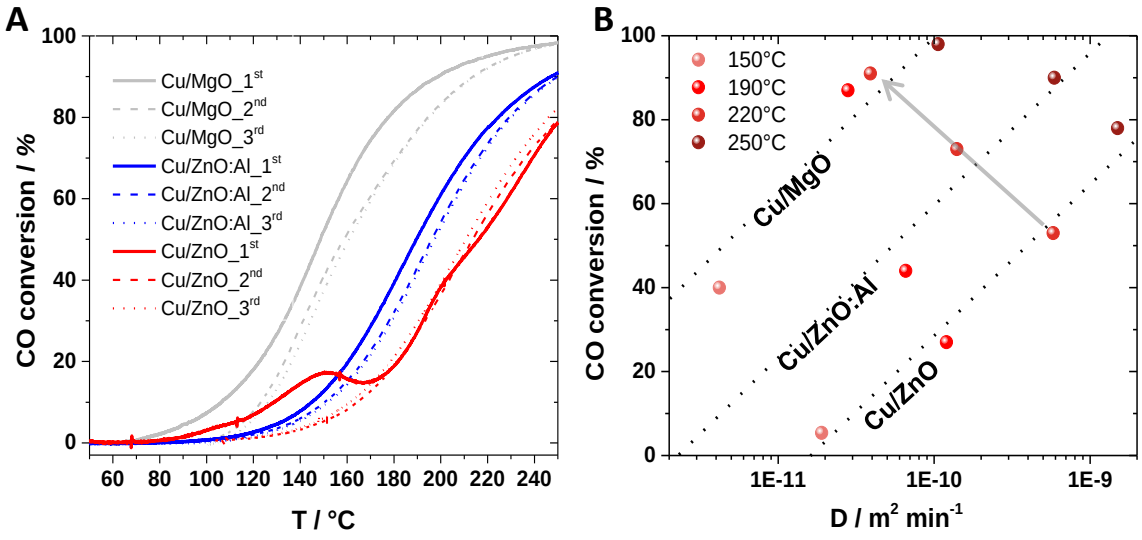

Figure 5. *Light-off curves in CO oxidation of Cu/MgO, Cu/ZnO and Cu/ZnO:Al catalysts with 3 consecutive cycles (A). Correlation of the CO oxidation performance and the corresponding diffusion coefficient (B).*

The relevance of the Cu oxidation state to the catalytic performance in CO-oxidation has been reported in an extensive surface science and kinetic study by Jernigan and Somorjai [58]. It was shown that the rate of reaction at 300°C decreased (Cu>Cu_2O>CuO) and the activation

energy rose with increasing Cu oxidation state. This observation agrees well with our results showing a decrease in activity with ongoing oxidation leading finally to a stable performance. This is experimentally supported by isothermal CO oxidation of Cu/ZnO (125°C, Figure S8A). After an oxidation-induced high activity event during the heating period, the performance is stable for 24 h time-on-stream. Re-reduction of the binary Cu/ZnO catalyst (Figure S8B) shows in the TPR profile a single event at low temperatures, attributed previously to nanostructured Cu_2O [59, 60]. The CO conversion (from cycle 2) at selected temperatures plotted as a function of the diffusion coefficient (log10 scale) elucidate an inverse correlation between the diffusion properties and the corresponding catalytic activities (Figure 5B, grey arrow highlights values at 220 °C). Due to the smaller oxygen diffusion coefficients of Cu/MgO and Cu/ZnO:Al the oxidation of Cu to nanostructured Cu_2O during the 1st cycle is slower and occurs over the whole temperature range (without "saddle-like" profile). This leads to a deactivation but stable performance for the subsequent 2nd and 3rd cycle. It seems that the current observation stems from a distinct stabilization effect on the Cu moieties as a result of an intimate interfacial contact to MgO and ZnO:Al supports [61] [62] [25], which prevents Cu from aggregation and fast oxidation. The oxygen diffusion induced sintering effects are irreversible indicated by the lower conversion in CO oxidation for the second cycle series (4th to 6th cycle, Fig. S9). Re-reducing the binary Cu/ZnO catalyst after the 3rd cycle restores again the low-temperature activity (oxidation induced "saddle-like" profile), but strongly shifted to higher temperatures (Fig. S9). This deactivation of the catalyst is justified by the applied red-ox cycles, which trigger phase separation processes [63].

The inverse correlation of oxygen diffusion and CO oxidation (coupled to multiple structural rearrangements) seems to be steered by the SMSI controlled interfacial contact, which is, influenced by electronic effects as well [44, 64]. In order to create a deeper understanding on the role of the Cu oxidation state under CO oxidation conditions (and SMSI in general) selected *in-situ* NEXAFS experiments were conducted. Starting from a completely reduced catalyst, under an atmosphere of 0.25 mbar ($CO:O_2$=2:1), Cu L_3-edge, Zn LMM Auger and work function measurements were performed. The oxidation state of Cu or Cu^0 to Cu oxide ratio (Cu_2O, CuO), respectively is quantified based on linear combination of Cu, Cu_2O, CuO reference measurements (Fig. S4).

Figure S10 A-C shows exemplarily the results of Cu/ZnO as function of the temperature under CO Oxidation conditions (catalytically active state, Fig. S10B). A non-linear change of the oxidation state of Cu (Table S3, as already observed for N_2O experiments, Fig. 3B) is interpreted as a competing role of temperature and gas phase (e.g. reductive character of CO).

The Zn LMM Auger spectra, at ~991 eV kinetic energy indicative for oxygen defects/vacancies [6], seems to be unaffected by the temperature (Fig. S10C). Figure 6A shows the Cu L_3-edge NEXAFS experiments of Cu/ZnO:Al at UHV conditions, before and during (at 25 and 250 °C, dwelled for 2h) the CO oxidation. In addition, the electronic work functions (from valence band and secondary electron cut-off measurements) were calculated. Under UHV conditions Cu is in the completely reduced state (see also Table S4), with a work function of 4.3 eV in agreement with Cu/MgO (4.3 eV, Figure S11A). This means that the work function seems to be independent of the semi-conducting (ZnO:Al) or insulating (MgO) character of the support, but, however, distinctly different to Cu powder reference measurements (3.2 eV, Fig. S11B). The difference to pure Cu might be explained by the highly dispersed nanostructured character of Cu and its intimate interfacial contact to the oxidic matrices (comparable work functions of ~4.7 eV) [65-68] also affecting strongly the electronic properties of the catalysts.[64, 67] Applying to Cu/ZnO:Al (or Cu/MgO and a Cu reference, Fig. S11) CO oxidation conditions (0.25 mbar), an incremental increase of the work function is observed, particularly as function of the temperature.

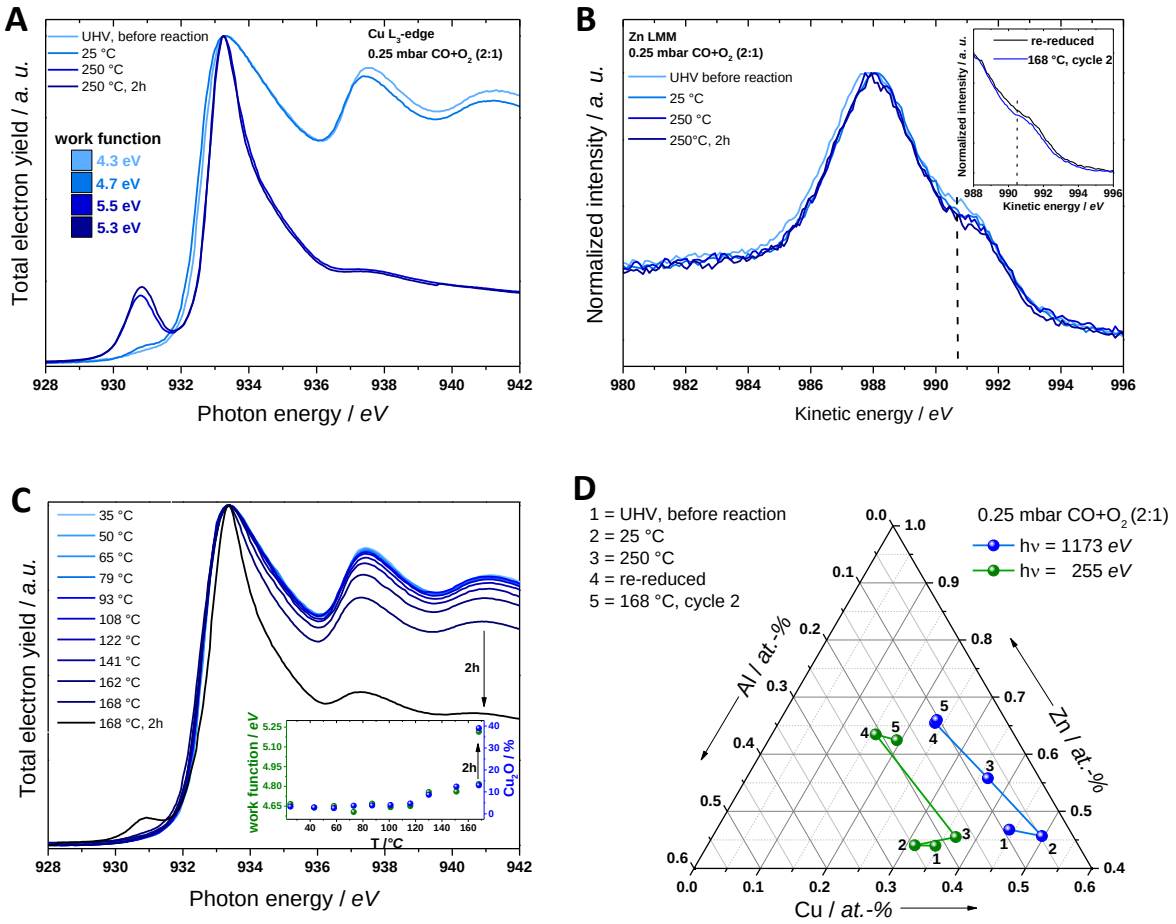

Figure 6. *Cu L_3-edge NEXAFS and work function measurements of Cu/ZnO:Al at various temperatures under 0.25 mbar CO:O_2=2:1 (A). Zn LMM Auger spectra at various conditions (B). Cu L_3-edge NEXAFS and work function measurements of a 2nd cycle CO oxidation (C). Elemental composition for different excitation energies and working states of the catalyst, nominal composition in at.%: 68 Cu, 29 Zn and 3 Al (D).*

The increase of the work function values is directly correlating to an increase in Cu_2O/CuO moieties (Table S4 and Table S3), finally leading to almost similar values (at 250 °C, 5.2-5.5 eV, Fig. 6A and S11). Since MgO and ZnO are mainly unaffected under these conditions, the work function values are dominated by Cu-oxide phases. This is confirmed by a 2nd CO oxidation cycle (after re-reduction) of Cu/ZnO:Al, directly evidencing a correlation between the work function measurements and amount of Cu_2O (inset Figure 6C, Table S4). The oxygen deficient character of ZnO:Al is indicated by the shoulder at ~991 eV in the Zn LMM Auger spectra (Figure 6B). In contact to CO/O_2 this shoulder is slightly decreasing (likely filled vacancies in ZnO), regenerated applying reductive conditions and decreases again under CO oxidation (inset Figure 6B, 2nd cycle). It is suggested that the dynamic character of the oxidation state of Cu (Table S4 and S3), the oxygen vacancies in ZnO:Al (Fig. 6B) and the change of the work functions (Fig. 6 A,C and Fig. S11) are coupled structural and electronic phenomena controlled by the metal-support-interaction. This is further corroborated by comparing the surface and near-surface elemental composition of Cu/ZnO:Al with (Figure 6D, see also Figure S13). The steps 1-5 describe an experimental sequence with different information depth. For both excitation energies of 255 eV (0.5 nm inelastic mean free path, green circles) and 1173 eV (2.3 nm inelastic mean free path, blue circles), an surface enrichment of Zn and Al is stronger pronounced (e.g. reduced state in UHV 35 at.% Cu at 255 eV, 45 at.% Cu at 1173 eV; nominal 69 at.% Cu). This is in excellent agreement with previous results of depth profiling by Schumann et al. reported for the reduced state[23]. With ongoing experimental sequence (CO oxidation from 25 to 250 °C, re-reduction and 2nd cycle), the surface becomes at first Al-enriched (likely phase separation tendencies of oxygen deficient ZnO:Al by surface oxidation, see also Table S4), then Cu-enriched (ongoing oxidation of Cu) and finally again Zn-enriched (re-reduction forms again a strongly Zn-enriched surface with less Al as dopant/part of the ZnO lattice). The most bulk sensitive measurement (blue circles) shows also remarkable changes in the elemental composition (from Cu- to Zn- enriched) resulting again in a strongly Zn/Al-enriched state. On the contrary, Cu/MgO exhibits a persistent Cu enrichment in both, surface and near-surface, regions for the series of conditions, featuring the strong and static character of the MgO support (Figure S14). These dynamics in elemental composition as function of temperature and gas phase [62] mirror the whole complexity of a metal/metal oxide catalyst

and its intriguing interfacial contact coupled to various electronic and structural adaptations also named as metal-support-interaction.

4. Conclusion and final remarks

A series of Cu/metal oxide (ZnO, ZnO:Al, MgO) catalysts was investigated by temperature dependent N_2O-RFC experiments. The determined oxygen diffusion coefficients and tendency of Cu_2O-layer formation are strongly influenced by the oxidic supports (e.g. removing the stabilizing character of the supports in impregnated samples leads to significantly higher diffusion coefficients). *In-situ* XRD measurements revealed that defects in Cu are more pronounced for dispersed Cu particles in ZnO:Al and MgO matrices. The more defective catalysts exhibit also a decreased tendency in Cu_2O-formation and smaller diffusion coefficients (in comparison to Cu/ZnO). It is assumed that the differently pronounced metal-support-interactions are responsible for differences in Cu particles, its microstructure and oxygen diffusion properties, respectively. This interpretation is supported by *in-situ* N_2O experiments (XRD and NEXAFS), evidencing more defective and strained Cu_2O domains upon oxidation and an estimated Cu_2O-layer thickness in fair agreement to the values obtained by oxygen diffusion experiments. This extends the role of metal-support-interactions, so far occurring at the metal-oxide interface during reduction/metal formation, towards the oxidation process of the metal and the corresponding oxygen diffusion properties (development of a Cu_2O front affected by the metal support interaction as represented by the Cu/($Cu^{\delta+}$-*O*)-ZnO or -*O*-MgO interface) [7, 8]. As a consequence, the calculated apparent activation energies of the oxygen diffusion process are also different. The E_a decrease with the oxygen diffusion coefficients and correlate inversely with the strength of the Cu support interaction, evidencing the probing character of the applied technique. Further, the calculated diffusion coefficients correlate inverse with the CO oxidation activities, as suitable probe reaction for SMSI. Isothermal reactivity and *in-situ* NEXAFS measurements identify the oxidation of Cu as deactivation phenomenon, leading for the Cu/ZnO system to a kind of "low-temperature activity" explained by the high oxygen diffusion coefficient. The diffusion-controlled oxidation of Cu and the strength of embedment and interaction to their matrices (ZnO, ZnO:Al, MgO) defines their reactivity. Besides the described structural influence of the metal-support-interaction, also the impact on the electronic structure has to be considered. The electronic work function of a Cu reference and supported Cu/ZnO:Al (or Cu/MgO) are significantly different, explained by the well dispersed, defective Cu nanostructures. The change of the work function is coupled to the amount of formed Cu_2O during CO oxidation, directly evidencing

the dominating character of the Cu-moieties on the electronic structure/properties. The dynamic character of the oxidation state (during CO oxidation and N_2O treatment) and the catalysts` structures are also visible in the elemental composition. As function of the temperature and gas phase, significant Zn and Al enrichment is detected, more pronounced on the surface. This evidences the complexity in describing and quantifying metal-support-interaction. However, the applicability of the extended N_2O titration test and the evaluation of the corresponding oxygen diffusion coefficients serve as suitable technique categorizing the metal-support-interaction. Beyond the quantification and kinetic analysis of the oxygen diffusion coefficients, this version of N_2O titration could be utilized as a rapid aging test for selected systems in terms of its resistivity/tendency to phase separation phenomena as a source of deactivation in general (e.g. recently identified as phase re-crystallization and segregation process) [7].

Acknowledgment

AT acknowledges Dr. Edward Kunkes and Prof. Dr. Malte Behrens for the discussions and ideas. EF acknowledges Dr. Maximilian Lamoth and Dr. Julia Schumann for the preparation of selected catalysts and Dr. Mark Greiner for data processing.

[1] D. 66136-1, Determination of the degree of dispersion of metals using gas chemisorption, Part:1 Principles, DIN, 2004.
[2] D. 66136-3, Detrmination of the degree of dispersion of metals using chemisorption, Part 3: Flow method, DIN, 2007.
[3] O. Hinrichsen, T. Genger, M. Muhler, Chemisorption of N2O and H2 for the Surface Determination of Copper Catalysts, Chemical Engineering & Technology, 23 (2000) 956-959.
[4] M.B. Fichtl, O. Hinrichsen, On the Temperature Programmed Desorption of Hydrogen from Polycrystalline Copper, Catalysis Letters, 144 (2014) 2114-2120.
[5] R. Chatterjee, S. Kuld, R. van den Berg, A. Chen, W. Shen, J.M. Christensen, A.D. Jensen, J. Sehested, Mapping Support Interactions in Copper Catalysts, Topics in Catalysis, 62 (2019) 649-659.
[6] S. Kuld, C. Conradsen, P.G. Moses, I. Chorkendorff, J. Sehested, Quantification of Zinc Atoms in a Surface Alloy on Copper in an Industrial-Type Methanol Synthesis Catalyst, Angewandte Chemie, (2014).
[7] T. Lunkenbein, F. Girgsdies, T. Kandemir, N. Thomas, M. Behrens, R. Schlogl, E. Frei, Bridging the Time Gap: A Copper/Zinc Oxide/Aluminum Oxide Catalyst for Methanol Synthesis Studied under Industrially Relevant Conditions and Time Scales, Angewandte Chemie, (2016).

[8] T. Lunkenbein, J. Schumann, M. Behrens, R. Schlogl, M.G. Willinger, Formation of a ZnO overlayer in industrial Cu/ZnO/Al2 O3 catalysts induced by strong metal-support interactions, Angewandte Chemie, 54 (2015) 4544-4548.
[9] M.B. Fichtl, J. Schumann, I. Kasatkin, N. Jacobsen, M. Behrens, R. Schlogl, M. Muhler, O. Hinrichsen, Counting of oxygen defects versus metal surface sites in methanol synthesis catalysts by different probe molecules, Angewandte Chemie, 53 (2014) 7043-7047.
[10] S. Sato, R. Takahashi, T. Sodesawa, K.-i. Yuma, Y. Obata, Distinction between Surface and Bulk Oxidation of Cu through N2O Decomposition, Journal of Catalysis, 196 (2000) 195-199.
[11] J.R. Jensen, T. Johannessen, H. Livbjerg, An improved N2O-method for measuring Cu-dispersion, Applied Catalysis A: General, 266 (2004) 117-122.
[12] J. Schumann, J. Kröhnert, E. Frei, R. Schlögl, A. Trunschke, IR-Spectroscopic Study on the Interface of Cu-Based Methanol Synthesis Catalysts: Evidence for the Formation of a ZnO Overlayer, Topics in Catalysis, 60 (2017) 1735-1743.
[13] H. Yoshida, T. Tsuruta, Y. Yazawa, T. Hattori, Support effect on oxidation resistance of precious metal catalysts as examined by N2O decomposition, Applied Catalysis A: General, 325 (2007) 50-56.
[14] H.V. Thang, S. Tosoni, G. Pacchioni, Evidence of Charge Transfer to Atomic and Molecular Adsorbates on ZnO/X(111) (X = Cu, Ag, Au) Ultrathin Films. Relevance for Cu/ZnO Catalysts, ACS Catalysis, 8 (2018) 4110-4119.
[15] A.T. Fromhold, Introduction to gas-solid reactions resulting in the formation of thin-film barrier layers, in: S. Amelinckx, R. Gevers, J. Nihoul (Eds.) Theory of Metal Oxidation, North-Holland Publishing Company, Netherlands, 1976, pp. 3-37.
[16] M.T. Greiner, T.E. Jones, B.E. Johnson, T.C.R. Rocha, Z.J. Wang, M. Armbrüster, M. Willinger, A. Knop-Gericke, R. Schlögl, The oxidation of copper catalysts during ethylene epoxidation, Physical Chemistry Chemical Physics, 17 (2015) 25073-25089.
[17] D. Bikaljevic, R. Rameshan, N. Köpfle, T. Götsch, E. Mühlegger, R. Schlögl, S. Penner, N. Memmel, B. Klötzer, Structural and kinetic aspects of CO oxidation on ZnOx-modified Cu surfaces, Applied Catalysis A: General, 572 (2019) 151-157.
[18] P. Kast, M. Friedrich, F. Girgsdies, J. Kröhnert, D. Teschner, T. Lunkenbein, M. Behrens, R. Schlögl, Strong metal-support interaction and alloying in Pd/ZnO catalysts for CO oxidation, Catalysis Today, 260 (2016) 21-31.
[19] P. Kast, M. Friedrich, D. Teschner, F. Girgsdies, T. Lunkenbein, R. Naumann d'Alnoncourt, M. Behrens, R. Schlögl, CO oxidation as a test reaction for strong metal–support interaction in nanostructured Pd/FeOx powder catalysts, Applied Catalysis A: General, 502 (2015) 8-17.
[20] M. Behrens, R. Schlögl, How to Prepare a Good Cu/ZnO Catalyst or the Role of Solid State Chemistry for the Synthesis of Nanostructured Catalysts, Zeitschrift für anorganische und allgemeine Chemie, 639 (2013) 2683-2695.
[21] M. Behrens, Meso- and nano-structuring of industrial Cu/ZnO/(Al2O3) catalysts, J. Catal., 267 (2009) 24-29.
[22] J. Schumann, A. Tarasov, N. Thomas, R. Schlögl, M. Behrens, Cu,Zn-based catalysts for methanol synthesis: On the effect of calcination conditions and the part of residual carbonates, Applied Catalysis A: General, 516 (2016) 117-126.
[23] J. Schumann, T. Lunkenbein, A. Tarasov, N. Thomas, R. Schlögl, M. Behrens, Synthesis and Characterisation of a Highly Active Cu/ZnO:Al Catalyst, ChemCatChem, 6 (2014) 2889-2897.
[24] J. Schumann, M. Eichelbaum, T. Lunkenbein, N. Thomas, M.C. Álvarez Galván, R. Schlögl, M. Behrens, Promoting Strong Metal Support Interaction: Doping ZnO for Enhanced Activity of Cu/ZnO:M (M = Al, Ga, Mg) Catalysts, ACS Catalysis, 5 (2015) 3260-3270.
[25] S. Zander, E.L. Kunkes, M.E. Schuster, J. Schumann, G. Weinberg, D. Teschner, N. Jacobsen, R. Schlogl, M. Behrens, The role of the oxide component in the development of copper composite catalysts for methanol synthesis, Angewandte Chemie, 52 (2013) 6536-6540.
[26] G.C. Chinchen, C.M. Hay, H.D. Vandervell, K.C. Waugh, The measurement of copper surface areas by reactive frontal chromatography, J. Catal., 103 (1987) 79-86.

[27] M. Behrens, S. Zander, P. Kurr, N. Jacobsen, J. Senker, G. Koch, T. Ressler, R.W. Fischer, R. Schlogl, Performance improvement of nanocatalysts by promoter-induced defects in the support material: methanol synthesis over Cu/ZnO:Al, Journal of the American Chemical Society, 135 (2013) 6061-6068.
[28] J. Lu, J.J. Bravo-Suárez, A. Takahashi, M. Haruta, S.T. Oyama, In situ UV–vis studies of the effect of particle size on the epoxidation of ethylene and propylene on supported silver catalysts with molecular oxygen, Journal of Catalysis, 232 (2005) 85-95.
[29] C. Wagner, Z. physik. Chem. (B), 21 (1933) 25.
[30] J. Bardeen, W.H. Brattain, W. Shockley, Investigation of Oxidation of Copper by Use of Radioactive Cu Tracer, The Journal of Chemical Physics, 14 (1946) 714-721.
[31] S.-i. Fujita, S. Matsumoto, N. Takezawa, Temperature programmed oxidation of Cu/ZnO catalysts with N2O: an attempt for characterization of copper catalysts, Catalysis Letters, 25 (1994) 29-36.
[32] A. Klyushin, Arrigo, R., Pfeifer, V., Jones, T., Velasco Vélez, J., & Knop-Gericke, A, Catalyst Electronic Surface Structure Under Gas and Liquid Environments., Elsevier2018.
[33] A. Knop‐Gericke, E. Kleimenov, M. Hävecker, R. Blume, D. Teschner, S. Zafeiratos, R. Schlögl, V.I. Bukhtiyarov, V.V. Kaichev, I.P. Prosvirin, A.I. Nizovskii, H. Bluhm, A. Barinov, P. Dudin, M. Kiskinova, Chapter 4 X‐Ray Photoelectron Spectroscopy for Investigation of Heterogeneous Catalytic Processes, Advances in Catalysis, Academic Press2009, pp. 213-272.
[34] M.L. Narula, V.B. Tare, W.L. LWorrell, Diffusivity and solubility of oxygen in solid copper using potentiostatic and potentiometric techniques, Metallurgical Transaction B, 14B (1983) 673-677.
[35] T.A. Ramanarayanan, W.L. Worrell, Overvoltage phenomena in electrochemical cells with oxygen-saturated copper electrodes, Metallurgical Transactions, 5 (1974) 1773-1777.
[36] E. Albert, R. Kircheim, Diffusivity of oxygen in copper, Scripta Metallurgica, 15 (1981) 673-677.
[37] M.W. Roberts, C.S. McKee, the intereaction of oxygen with metal surfaces, Chemistry of Metal-Gas Interface, Clarendon Press Oxford1978, pp. 442-448.
[38] L. Zwiener, F. Girgsdies, D. Brennecke, D. Teschner, A.G.F. Machoke, R. Schlögl, E. Frei, Evolution of zincian malachite synthesis by low temperature co-precipitation and its catalytic impact on the methanol synthesis, Applied Catalysis B: Environmental, 249 (2019) 218-226.
[39] J.J.F. Scholten, J.A. Konvalinka, Reaction of nitrous oxide with copper surfaces. Application to the determination of free-copper surface areas, Transactions of the Faraday Society, 65 (1969) 2465.
[40] W.D. Kingery, H.K. Bowen, D.R. Uhlmann, Introduction to Ceramics, Wiley, New York, 1976, pp. 217.
[41] J. Crank, Infinite and semi-infinite media, The Methematics of Diffusion, Clarendon Press, Oxford, 1975, pp. 28-43.
[42] J. Schumann, T. Lunkenbein, A. Tarasov, N. Thomas, R. Schlögl, M. Behrens, Synthesis and Characterisation of a Highly Active Cu/ZnO:Al Catalyst, ChemCatChem, 6 (2014) 2889-2897.
[43] C. Wagner, K. Grünewald, Beitrag zur Theorie des Anlaufvorganges., Z. physik. Chem. (B), 40 (1938) 455-475.
[44] E. Frei, A. Gaur, H. Lichtenberg, C. Heine, M. Friedrich, M. Greiner, T. Lunkenbein, J.-D. Grunwaldt, R. Schlögl, Activating a Cu/ZnO : Al Catalyst – Much More than Reduction: Decomposition, Self-Doping and Polymorphism, ChemCatChem, 11 (2019) 1587-1592.
[45] J. T. Ranney, D. E. Starr, J. E. Musgrove, D. J. Bald, C. T. Campbell, A microcalorimetric study of the heat of adsorption of copper on well-defined oxide thin film surfaces: MgO(100), p(2×1) oxide on Mo(100) and disordered W oxide, Faraday Discussions, 114 (1999) 195-208.
[46] L.V. Koplitz, O. Dulub, U. Diebold, STM Study of Copper Growth on ZnO(0001)−Zn and ZnO(000$\bar{1}$)−O Surfaces, The Journal of Physical Chemistry B, 107 (2003) 10583-10590.
[47] P.L. Hansen, J.B. Wagner, S. Helveg, J.R. Rostrup-Nielsen, B.S. Clausen, H. Topsøe, Atom-Resolved Imaging of Dynamic Shape Changes in Supported Copper Nanocrystals, Science, 295 (2002) 2053-2055.

[48] I. Kasatkin, B. Kniep, T. Ressler, Cu/ZnO and Cu/ZrO2 interactions studied by contact angle measurement with TEM, Physical Chemistry Chemical Physics, 9 (2007) 878-883.
[49] M.A. Brown, E. Carrasco, M. Sterrer, H.-J. Freund, Enhanced Stability of Gold Clusters Supported on Hydroxylated MgO(001) Surfaces, Journal of the American Chemical Society, 132 (2010) 4064-4065.
[50] M.A. Brown, Y. Fujimori, F. Ringleb, X. Shao, F. Stavale, N. Nilius, M. Sterrer, H.-J. Freund, Oxidation of Au by Surface OH: Nucleation and Electronic Structure of Gold on Hydroxylated MgO(001), Journal of the American Chemical Society, 133 (2011) 10668-10676.
[51] D.E. Starr, S.F. Diaz, J.E. Musgrove, J.T. Ranney, D.J. Bald, L. Nelen, H. Ihm, C.T. Campbell, Heat of adsorption of Cu and Pb on hydroxyl-covered MgO(100), Surface Science, 515 (2002) 13-20.
[52] T.A. Ramanarayanan, R.A. Rapp, The diffusivity and solubility of oxygen in liquid tin and solid silver and the diffusivity, Metallurgical Transactions, 3 (1972) 3239-3246.
[53] V.M. Gryaznov, S.G. Gul´yanova, S. Kanizius, Diffusion of Oxygen through a Silver Membrane, Russian Journal of Physical Chemistry, 47 (1973) 1517-1518.
[54] M.T. Greiner, T.E. Jones, B.E. Johnson, T.C. Rocha, Z.J. Wang, M. Armbruster, M. Willinger, A. Knop-Gericke, R. Schlogl, The oxidation of copper catalysts during ethylene epoxidation, Phys Chem Chem Phys, 17 (2015) 25073-25089.
[55] R.M. Dell, F.S. Stone, P.F. Tiley, The adsorption of oxygen and other gases on copper, Transactions of the Faraday Society, 49 (1953) 195-201.
[56] R.L. Pastorek, R.A. Rapp, Trans. AIME, 245 (1969) 1711.
[57] L. Luo, Y. Nian, S. Wang, Y. He, Y. Han, C. Wang, Z. Dong, Real time atomic-scale visualization of Cu surface reversible activation in CO oxidation reaction, Angewandte Chemie, n/a.
[58] G.G. Jernigan, G.A. Somorjai, Carbon Monoxide Oxidation over Three Different Oxidation States of Copper: Metallic Copper, Copper (I) Oxide, and Copper (II) Oxide - A Surface Science and Kinetic Study, Journal of Catalysis, 147 (1994) 567-577.
[59] S. Kühl, A. Tarasov, S. Zander, I. Kasatkin, M. Behrens, Cu-Based Catalyst Resulting from a Cu,Zn,Al Hydrotalcite-Like Compound: A Microstructural, Thermoanalytical, and In Situ XAS Study, Chemistry - A European Journal, 20 (2014) 3782-3792.
[60] C. Álvarez Galván, J. Schumann, M. Behrens, J.L.G. Fierro, R. Schlögl, E. Frei, Reverse water-gas shift reaction at the Cu/ZnO interface: Influence of the Cu/Zn ratio on structure-activity correlations, Applied Catalysis B: Environmental, 195 (2016) 104-111.
[61] M. Behrens, F. Studt, I. Kasatkin, S. Kuhl, M. Havecker, F. Abild-Pedersen, S. Zander, F. Girgsdies, P. Kurr, B.L. Kniep, M. Tovar, R.W. Fischer, J.K. Norskov, R. Schlogl, The active site of methanol synthesis over Cu/ZnO/Al2O3 industrial catalysts, Science, 336 (2012) 893-897.
[62] J.D. Grunwaldt, A.M. Molenbroek, N.Y. Topsøe, H. Topsøe, B.S. Clausen, In Situ Investigations of Structural Changes in Cu/ZnO Catalysts, Journal of Catalysis, 194 (2000) 452-460.
[63] A.D. Smigelskas, E.O. Kirkendall, Zinc Diffusion in Alpha Brass, Trans. AIME, 171 (1947) 130-142.
[64] I. Beinik, M. Hellström, T.N. Jensen, P. Broqvist, J.V. Lauritsen, Enhanced wetting of Cu on ZnO by migration of subsurface oxygen vacancies, Nature Communications, 6 (2015) 8845.
[65] T. Su, H. Zhang, Electrical Study of Trapped Charges in Copper-Doped Zinc Oxide Films by Scanning Probe Microscopy for Nonvolatile Memory Applications, PLOS ONE, 12 (2017) e0171050.
[66] C. Thu, P. Ehrenreich, K.K. Wong, E. Zimmermann, J. Dorman, W. Wang, A. Fakharuddin, M. Putnik, C. Drivas, A. Koutsoubelitis, M. Vasilopoulou, L.C. Palilis, S. Kennou, J. Kalb, T. Pfadler, L. Schmidt-Mende, Role of the Metal-Oxide Work Function on Photocurrent Generation in Hybrid Solar Cells, Scientific Reports, 8 (2018) 3559.
[67] S.S. Wilson, J.P. Bosco, Y. Tolstova, D.O. Scanlon, G.W. Watson, H.A. Atwater, Interface stoichiometry control to improve device voltage and modify band alignment in ZnO/Cu2O heterojunction solar cells, Energy & Environmental Science, 7 (2014) 3606-3610.
[68] E.H. Choi, J.Y. Lim, S.O. Kang, H.S. Uhm, Measurement of Work Function at MgO Crystal Surface by the γ-Focused Ion Beam System, Japanese Journal of Applied Physics, 41 (2002) L1006-L1009.

TOC

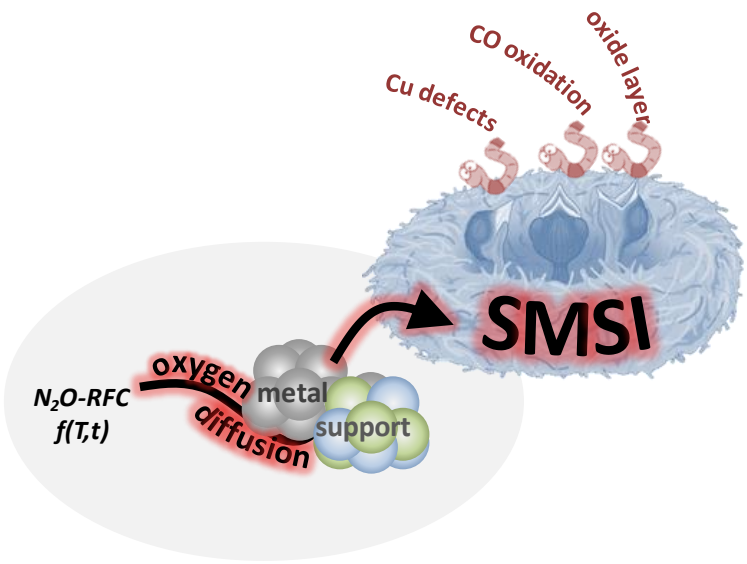
oxide layer
CO oxidation
Cu defects
SMSI
oxygen
diffusion
metal
support
N_2O-RFC
f(T,t)